Lipari, G., & Szabo, A. (1982b) *J. Am. Chem. Soc. 104*, 4559-4570.
Magde, D., Zappala, M., Knox, W. H., & Nordlund, T. H. (1983) *J. Chem. Phys. 87*, 3286-3288.
Millar, D. P., Robbins, R. J., & Zewail, A. H. (1981) *J. Chem. Phys. 76*, 2080-2094.
Millero, F. J., Dexter, R., & Hoff, E. (1971) *J. Chem. Eng. Data 16*, 85-87.
Mirau, P. A., & Kearns, D. R. (1983) *Biochemistry 23*, 5439-5446.
Mirau, P. A., Behling, R. W., & Kearns, D. R. (1985) *Biochemistry 24*, 6200-6211.
Perrin, F. (1934) *J. Phys. Radium 5*, 497-510.
Perrin, F. (1936) *J. Phys. Radium 7*, 1-11.
Saenger, W. (1984) *Principles of Nucleic Acid Structure*, Springer-Verlag, New York.
Schurr, J. M. (1984) *Chem. Phys. 84*, 71-96.
Schurr, J. M., & Fujimoto, B. S. (1988) *Biopolymers 27*, 1543-1569.
Shindo, H., Hiyama, Y., Siddhartha, R., Cohen, J. S., & Torchia, D. A. (1987) *Bull. Chem. Soc. Jpn. 60*, 1631-1640.
Spiess, H. W. (1978) Dynamic NMR Spectroscopy, *Basic Princ. Prog. NMR 15*, 54-214.
Tirado, M. M., & Garcia de la Torre, J. (1979) *J. Chem. Phys. 71*, 2581-2587.
Tirado, M. M., & Garcia de la Torre, J. (1980) *J. Chem. Phys. 73*, 1986-1993.
Tirado, M. M., Lopez Martinez, M. C., & Garcia de la Torre, J. (1984a) *J. Chem. Phys. 81*, 2047-2052.
Tirado, M. M., Lopez Martinez, M. C., & Garcia de la Torre, J. (1984b) *Biopolymers 23*, 611-615.
van Cittert, P. H. (1931) *Z. Phys. 69*, 298.
Wang, C. C., & Pecora, R. (1980) *J. Chem. Phys. 72*, 5333-5340.
Williamson, J. R. (1988) Ph.D. Thesis, Stanford University.
Williamson, J. R., & Boxer, S. G. (1989) *Biochemistry 28*, 2819-2831.
Woessner, D. E. (1962) *J. Chem. Phys. 37*, 647-654.
Wu, P., Fujimoto, B. S., & Schurr, J. M. (1987) *Biopolymers 26*, 1463-1488.
Wüthrich, K. (1986) *NMR of Proteins and Nucleic Acids*, Wiley, New York.
Yoshizaki, T., & Yamakawa, H. (1980) *J. Chem. Phys. 72*, 57-69.
Youngren, G. K., & Acrivos, A. (1976) *J. Chem. Phys. 63*, 3846-3848.

Synthesis and Characterization of *trans*-[$Pt(NH_3)_2Cl_2$] Adducts of d(CCTCGAGTCTCC)·d(GGAGACTCGAGG)†

Christopher A. Lepre, Laurent Chassot, Catherine E. Costello, and Stephen J. Lippard*
Department of Chemistry, Massachusetts Institute of Technology, Cambridge, Massachusetts 02139
Received May 24, 1989; Revised Manuscript Received August 29, 1989

ABSTRACT: The reaction of *trans*-diamminedichloroplatinum(II) (*trans*-DDP), the inactive isomer of the anticancer drug cisplatin, with the single-stranded deoxydodecanucleotide d(CCTCGAGTCTCC) in aqueous solution at 37 °C was monitored by reversed-phase HPLC. Consumption of the dodecamer follows pseudo-first-order reaction kinetics with a rate constant of 1.25 (4) × 10^{-4} s^{-1}. Two intermediates, shown to be monofunctional adducts in which Pt is coordinated to the guanine N7 positions, were trapped with $NH_4(HCO_3)$ and identified by enzymatic degradation analysis. These monofunctional adducts and a third, less abundant, one are rapidly removed from the DNA by thiourea under mild conditions. When allowed to react further, the monofunctional intermediates formed a single main product that was characterized by ^1H NMR spectroscopy and enzymatic digestion as the bifunctional 1,3-intrastrand cross-link *trans*-[$Pt(NH_3)_2${d(CCTCGAGTCTCC)-*N7-G(5)*,*N7-G(7)*}]. Binding of the *trans*-$\{Pt(NH_3)_2\}^{2+}$ moiety to the guanosine N7 positions decreases the pK_a at N1 and leads to destacking of the intervening A(6) base. The double-stranded *trans*-DDP-modified and unmodified DNAs were obtained by annealing the complementary strand to the corresponding single strands and then studied by ^{31}P and ^1H NMR and UV spectroscopy. *trans*-DDP binding does not induce large changes in the O–P–O bond or torsional angles of the phosphodiester linkages in the duplex, nor does it significantly alter the UV melting temperature. *trans*-DDP binding does, however, cause the imino protons of the platinated duplex to exchange rapidly with solvent by 50 °C, a phenomenon that occurs at 65 °C for the unmodified duplex. A structural model for the platinated double-stranded oligonucleotide was generated through molecular dynamics calculations. This model reveals that the *trans*-DDP bifunctional adduct can be accommodated within the double helix with minimal distortion of the O–P–O angles and only local disruption of base pairing and destacking of the platinated bases. The model also predicts hydrogen bond formation involving coordinated ammine ligands that bridge the two strands.

The anticancer drug *cis*-diamminedichloroplatinum(II) (cisplatin, or *cis*-DDP) binds to DNA, inactivating it as a template for replication and transcription [for reviews see Pinto and Lippard (1985a), Lippard (1987), Reedijk (1987), Eastman (1987), Sherman and Lippard (1987) and Roberts (1988)]. The clinically ineffective trans isomer also binds DNA, forming adducts that terminate replication both in vivo

† We thank the Swiss National Science Foundation for a Postdoctoral Fellowship (to L.C.).

0006-2960/90/0429-811$02.50/0

and in vitro (Harder et al., 1976; Pinto & Lippard, 1985b; Gralla et al., 1987; Villani et al., 1988). Both *cis*- and *trans*-DDP bind preferentially to purine N7 positions, producing monofunctional adducts that subsequently close to bifunctional lesions. Recent quantitative ^{195}Pt NMR studies of these reactions reveal similar kinetic parameters for binding of the two isomers to both single- and double-stranded DNA (D. P. Bancroft, C. A. Lepre, and S. J. Lippard, unpublished results).

Despite these similarities, *cis*- and *trans*-DDP differ in the nature of their bifunctional adducts. The cis isomer forms predominantly 1,2-intrastrand cross-links between adjacent guanosine nucleosides both in vitro (Pinto & Lippard, 1985b; Fichtinger-Schepman et al., 1985; Eastman, 1987; Hemminki & Thilly, 1988) and in vivo (Fichtinger-Schepman et al., 1988a). The trans isomer, however, is stereochemically incapable of making 1,2-intrastrand cross-links (Cohen, et al., 1980). Instead, it forms 1,3-intrastrand adducts in vitro, primarily at d(GNG) and d(ANG) sequences where N is any nucleotide (Pinto & Lippard, 1985b; Lepre, et al., 1987). Quantitation indicates that 90% of *trans*-DDP adducts contain 1,3 or longer range dG–Pt–dG and dG–Pt–dC cross-links (Eastman et al., 1988). Since both 1,2- and 1,3-intrastrand cross-links inhibit replication, it has been postulated that the different biological activities of the two isomers may result from selective removal of structurally different *trans*-DDP adducts from DNA. Both enzymatic and chemical mechanisms, including removal of monofunctional *trans*-DDP adducts, have been considered for such a process (Ciccarelli et al., 1985; Eastman & Barry, 1987).

In order to understand the biological processing of platinum–DNA adducts, it is highly desirable to have detailed information about their stereochemistry. Most of the structural information currently available pertains to the cis isomer, with only a few structural investigations of *trans*-DDP–DNA adducts having been reported. NMR studies of the *trans*-DDP-modified oligonucleotides d(GTG) (van der Veer et al., 1986), d(GCG) (Gibson & Lippard, 1987), and d(AGGCCT) (Lepre et al., 1987) revealed formation of 1,3-intrastrand cross-links that destack the central base, distort the backbone, and cause the deoxyribose ring of the coordinated 5′-nucleoside to adopt an N conformation. Such single-stranded adducts afford incomplete information, however, since they cannot model the constraints of a double helix. Moreover, the extent of duplex disruption induced by formation of *trans*-DDP 1,3-intrastrand cross-links has been insufficiently explored.

A principal objective of the work reported here has been to characterize structurally the major *trans*-$\{Pt(NH_3)_2\}^{2+}$ 1,3-intrastrand d(GNG) cross-link built into double-stranded DNA and to compare the structure and stability of the platinated duplex to the unplatinated form. It was also of interest to identify preferred sites of formation of *trans*-DDP monofunctional adducts. In addition to fulfilling these objectives, the present work provides the first detailed geometric model for the *trans*-$\{Pt(NH_3)_2\}^{2+}$ 1,3-intrastrand cross-link on DNA as generated through molecular dynamics calculations. These results should be of value not only to investigators in the platinum anticancer drug area but also to those concerned in general with the structural chemistry of DNA damaging agents.

Materials and Methods

Synthesis of trans-[Pt(NH$_3$)$_2$\{d(CCTCGAGTCTCC)-N7-G(5),N7-G(7)\}]. Oligodeoxydodecanucleotides were synthesized by means of β-cyanoethyl phosphoramidite methodology (Sinha, 1983) and purified by anion-exchange liquid chromatography and reversed-phase HPLC. The purified oligonucleotides were converted to the sodium salt in some cases by passage through Dowex 50W (Sigma) cation-exchange resin. The sequence and composition of the dodecamers were confirmed by HPLC analysis of their enzymatic digests using an adaptation of literature methods (Eastman, 1986), and by negative ion fast atom bombardment mass spectrometry employing the method of Grotjan et al. (1985). Experimental protocols and details of the FABMS and MS/MS analysis are available as supplementary material.

In a typical synthesis of *trans*-[Pt(NH$_3$)$_2$\{d-(CCTCGAGTCTCC)-*N7-G(5),N7-G(7)*\}], 1.3 equiv of *trans*-DDP dissolved in distilled water at 60 °C were added to 1.01 μmol of d(CCTCGAGTCTCC) in water at a strand concentration of 0.067 mM. The pH of the solution was adjusted to 3.0 with metal-free HNO_3 (Ultrapure), and then the reaction was allowed to proceed for 18–20 h at 37 °C. The progress of the reaction was monitored by reversed-phase HPLC using a Waters μ Bondapak C_{18} column and a 30-min linear gradient of 8.5–15% acetonitrile in 0.1 M ammonium acetate buffer at pH 6.5. The mixture was frozen and lyophilized and the bifunctionally coordinated product purified by reversed-phase HPLC as described above. The volatile ammonium acetate salt was removed by repeatedly redissolving the sample in water and lyophilizing to dryness.

Characterization of trans-[Pt(NH$_3$)$_2$\{d-(CCTCGAGTCTCC)-N7-G(5),N7-G(7)\}]. ^1H NMR spectra of d(CCTCGAGTCTCC) and *trans*-[Pt(NH$_3$)$_2$\{d-(CCTCGAGTCTCC)-*N7-G(5),N7-G(7)*\}] were acquired at 499.8 MHz on a Varian VXR-500 spectrometer. Spectra were obtained with 1 mM samples in D_2O at 35 °C after first selectively presaturating the residual HDO resonance (appearing at 4.66 ppm at pH 7) at 47 dB for between 1 and 4 s. Data were processed with 1-Hz exponential line broadening to improve signal to noise. Chemical shifts were determined by using internal tetramethylammonium chloride (TMAC) at 3.180 ppm and are reported relative to DSS. For chemical shift measurements as a function of pD, the pD was adjusted with small aliquots of 2%, 4%, or 8% NaOD and DCl (Aldrich). The reported pD was the average of the values measured both before and after acquiring each spectrum. No correction was made for the deuterium isotope effect (Glasoe & Long, 1960). pK_a values reported correspond to midpoints of the sigmoidal titration curves.

The number of platinum atoms bound per dodecamer strand was determined from the ratio of platinum and dodecamer concentrations obtained by atomic absorption and UV spectroscopies. An extinction coefficient of 102 300 L/(mol·cm) at 260 nm was calculated for d(CCTCGAGTCTCC) (Fasman, 1975). Atomic absorption spectroscopy was carried out, after dilution, on the same samples by using a Varian AA-1475 spectrometer equipped with GTA-95 graphite furnace and auto sampler.

Binding sites of *trans*-DDP on d(CCTCGAGTCTCC) were also determined by enzymatic digestion of the platinated oligonucleotide, using the protocol described in the supplementary material. HPLC profiles are shown and discussed under Results. The HPLC peak corresponding to *trans*-$[Pt(NH_3)_2(dG)_2]^{2+}$ in the digestion mixture of *trans*-[Pt-(NH$_3$)$_2$\{d(CCTCGAGTCTCC)-*N7-G(5),N7-G(7)*\}] was identified by coinjection with the model complex *trans*-[Pt-(NH$_3$)$_2$(dG)$_2$]$^{2+}$ (vide infra); the synthesis and characterization by ^1H NMR and FABMS of this model complex are described in the supplementary material.

Studies of Monofunctional Adducts. Monofunctional adducts formed during the reaction between *trans*-DDP and d(CCTCGAGTCTCC) were trapped as the $\{Pt(NH_3)_3\}^{2+}$ species by employing the method of Fichtinger-Schepman et al. (1984, 1988a). In a typical determination, 0.0965 μmol of dry, HPLC-purified dodecamer was dissolved in 500 μL of distilled, deionized water (pH 5.0), to a final dodecamer concentration of 193 μM. To this solution was added 13.3 μl of freshly dissolved *trans*-DDP, 5.4 mg in 5.0 mL of DMF, giving a final ratio of 1.2 Pt per strand (2.6% DMF). The reaction mixture was then incubated at 37 °C until the monofunctional adducts were at their maximum concentration (at 3.5–4 h). To quench the reaction, 1.0 M NH_4HCO_3 was added to a final concentration of 0.2 M and pH 8, and the solution was incubated overnight at 37 °C. As described under Results, the products of this reaction were identical with those obtained from the reaction of $[Pt(NH_3)_3Cl]Cl$ with d(CCTCGAGTCTCC). The synthesis and characterization of $[Pt(NH_3)_3Cl]Cl$ are described in the supplementary material. Reactions with thiourea were carried out by allowing *trans*-DDP to react with the dodecamer to form monoadducts as described above, at which time small aliquots of fresh 1.0 M aqueous thiourea (Sigma, recrystallized solid stored at −20 °C) were added to give the desired final concentration.

In order to determine the binding sites of platinum in the monofunctional adducts, triammine monoadducts were generated in sufficient quantities for enzymatic digestion analysis by reaction of $[Pt(NH_3)_3Cl]Cl$ with d(CCTCGAGTCTCC). Recrystallized $[Pt(NH_3)_3Cl]Cl$ (30.6 μg) was dissolved in 500 μL of distilled, deionized water and added to 0.0965 μmol of dry dodecamer to give a final ratio of 1.0 Pt per strand and then was allowed to react at 37 °C for 24 h. The resulting stable triammine monoadducts were purified by reversed-phase HPLC and the $\{Pt(NH_3)_3\}^{2+}$ binding sites were determined by enzymatic digestion analysis. The $[Pt(NH_3)_3(dG)]^{2+}$ peak in the HPLC elution profile was identified by coinjection with synthetic $[Pt(NH_3)_3(dG)]^{2+}$, the preparation and characterization of which by ^1H NMR and FABMS are described in the supplementary material.

UV Melting Studies. Duplex oligonucleotide samples were prepared by allowing 0.5 OD each of purified d(CCTCGAGTCTCC) and *trans*-$[Pt(NH_3)_2\{$d(CCTCGAGTCTCC)-*N7-G(5),N7-G(7)*$\}]$ to anneal with 0.5 OD of the complementary strand in 800 μL of 0.1 M KH_2PO_4 (pH 7.0). The solution was mixed, heated to 85 °C, and allowed to cool slowly to 0 °C. UV melting curves were measured with buffer solution in the reference cell. The temperature of the sample cells was controlled by a circulating mixture of 40:60 methanol/water and measured in the sample cell with a thermocouple. The temperature was increased from 15 to 85 °C at a rate of 0.2 °C/min. Melting temperatures, determined either from the midpoints of sigmoidal plots of absorbance vs temperature or by the maxima of dA/dT vs T plots, were identical and are estimated to have an error of ±3 °C.

^1H and ^{31}P NMR Spectroscopic Studies. Duplex oligonucleotide samples used for NMR studies contained 0.9 μmol each of single strand and complement in 800 μL of 90% H_2O and 10% D_2O containing 0.1 M NaCl, 27 μM Na_2EDTA (pH 7), and a trace of TMAC as an internal reference. Prior to the experiments, samples were heated to 85 °C for 5–10 min and then cooled slowly to 10 °C.

The temperature dependence of the exchangeable base proton resonances was determined at 499.8 MHz while frequency locked on internal D_2O. At each temperature value, 256 transients were accumulated over a 10000-Hz sweep width, with a total recycle time of 1.2 s. A 90° composite binomial 1–3–3–1 pulse sequence (Hore, 1983) was employed to maximize the signal in the region of the imino resonances while suppressing the signal due to bulk water. After allowing 15 min at each new temperature value for the system to reach thermal equilibrium, the probe was tuned and the field shimmed before acquiring spectra. Free induction decays were weighted with a 2-Hz exponential line broadening factor to improve the signal-to-noise ratio and processed by standard Fourier transform techniques.

Temperature-dependent ^{31}P NMR spectra of platinated and unplatinated duplexes were acquired at 202.3 MHz. Samples used previously for the ^1H NMR studies were lyophilized to dryness and redissolved in 800 μL of D_2O (99.8%, Aldrich) to give a final concentration of 0.1 M NaCl and 27 μM Na_2EDTA, pH 7. After adding a trace of trimethyl phosphate (TMP) as internal reference (δ = 0.0 ppm), samples were annealed by heating to 90 °C for 5–10 min and slowly cooling to 4 °C. At each temperature value, 1024 or 2048 free induction decays were acquired over a 2642-Hz sweep width by using a 90° pulse, while frequency locked on internal D_2O. The total recycle time was 1.6 s. Heteronuclear proton broad-band decoupling was applied continuously while employing low-pass filtering to prevent interference with the lock or observe channels. Data were weighted with a 3-Hz exponential line broadening factor and processed by standard Fourier transform techniques.

Molecular Dynamics Calculations. The force field used was that of CHARMM (Nilsson & Karplus, 1986) and was carried out on a Convex C1 computer. The model included all heavy atoms and all polar hydrogens involved in hydrogen bonding; remaining hydrogens were treated as part of the heavy atom to which they are attached (extended atom model). Parameters for *trans*-$\{Pt(NH_3)_2\}^{2+}$ were taken from the force field derived for *cis*-$\{Pt(NH_3)_2\}^{2+}$, to be published elsewhere (L. Chassot, M. J. Field, M. Krauss, S. J. Lippard, and M. Karplus, unpublished results). An r-dependent dielectric factor, having a nonbond cutoff switching function applied between 11.5 and 12.5 Å and a cutoff for hydrogen bonds between 3.5 and 4.0 Å, was used in all calculations. Integrations of Newton's equations of motion were performed by using the Langevin algorithm with a friction coefficient of 60 ps^{-1}. SHAKE was used to restrain covalent bonds involving hydrogen, allowing a time step of 0.002 ps to be used.

The B-DNA helix was generated by the method of Arnott et al. (1976). The starting platinated oligonucleotide structure was obtained with the help of an IRIS 3030 graphics system and molecular mechanics. The sequence pGpApG was extracted from the dodecamer d(CCTCG*AG*TCTCC·d(GGAGACTCGAGG), and the *trans*-diammineplatinum(II) residue was inserted between the two guanine bases marked by an asterisk. The Pt–N7 distances were reduced by rotating the base and glycosidic bond portions around an axis passing through C1′. The central adenine base was moved aside from the platinum center in the same way. In order to relax the structure without altering the backbone, a short minimization was performed without the electrostatic term. The platinated segment was then inserted into its original position. Minimization of the central part of the modified dodecamer via 300 adopted basis Newton–Raphson (ABNR) steps generated the starting coordinates. From this strucure a molecular dynamics simulation of 40 ps was performed. The initial 8–10 ps of the simulations, during which the potential energy of the system was relaxing, was considered the equilibration period,

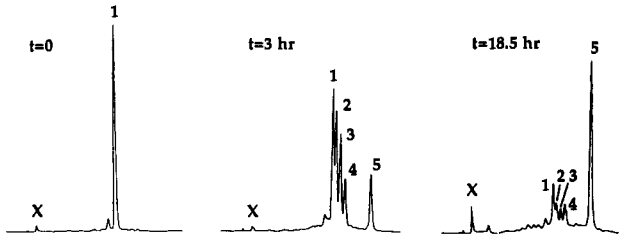

FIGURE 1: Reversed-phase HPLC elution profiles obtained during the course of the reaction between *trans*-DDP and d(CCTCGAGTCTCC) at 37 °C, in distilled water, pH 3. Peak 1 is unreacted d(CCTCGAGTCTCC); peaks 2–4 are monofunctional adducts; peak 5 is *trans*-[$Pt(NH_3)_2$\{d(CCTCGAGTCTCC)-*N7-G(5),N7-G(7)*\}] (product B1). The peak marked by "X" contains low molecular weight species that elute in the void volume of the HPLC column. Reaction times are (left) zero, (center) 3, and (right) 18.5 h. The DNA strand concentration is 70 μM, with 1.3 Pt added per strand.

after which a stable potential energy was achieved. The coordinates were saved every 0.1 ps during the last 20 ps and time-averaged. The molecular dynamics time-averaged structure was subjected to 500 ABNR energy-minimization steps with gradually decreasing harmonic constraint of the initial atomic positions prior to examination.

Results

Reaction of trans-DDP with d(CCTCGAGTCTCC). The reaction of *trans*-DDP with a duplex oligonucleotide comprised of multiple binding sites is expected to give a complex mixture of products. In order to simplify the preparation of the target dodecamer duplex, the platinated strand was first synthesized, purified, and characterized before annealing to the unmodified complementary strand. The base sequence of the platinated strand was selected to facilitate unique binding of *trans*-DDP to form a G-N7,G-N7 1,3-intrastrand cross-link. The d(GAG) target was centrally located and flanked by GC-rich sequences to maximize the melting temperature of the platinated duplex. Two G·C base pairs, positioned at the 3′ and 5′ termini of the sequence, limit transient base pair opening, or "fraying", at the ends of the duplex (Kan et al., 1975; Borer et al., 1975; Patel, 1978; Patel et al., 1982a,b; Fritzsche et al., 1983). In addition, the *Xho*I restriction endonuclease recognition sequence, d(CTCGAG) (Gingeras et al., 1978), was incorporated to facilitate future biological studies. The numbering scheme (5′ to 3′ direction) of the duplex is shown:

C(1) - C(2) - T(3) - C(4) - G(5) - A(6) - G(7) - T(8) - C(9) - T(10) - C(11) - C(12)
G(24) - G(23) - A(22) - G(21) - C(20) - T(19) - C(18) - A(17) - G(16) - A(15) - G(14) - G(13)

Reaction of the single-stranded dodecamer with *trans*-DDP was conducted at pH 3 in order to preclude adduct formation at A(6). Protonation of adenine N1 (pK_a = 3.8) blocks platinum binding by reducing the nucleophilicity of the N7 position. Platination at higher pH gave a variety of final products. The reaction time course at pH 3, as followed by reversed-phase HPLC, is shown in Figure 1. Three intermediate species form which elute immediately after unreacted dodecamer. Two of these intermediates, identified as monofunctional adducts at G-N7 (vide infra), are formed relatively rapidly, reaching a maximum concentration near 3.5 h, while the third forms more slowly, reaching its maximum concentration near 8 h.

Monofunctional intermediates slowly convert into one predominant bifunctional adduct that elutes late in the HPLC solvent gradient. No species elute under more hydrophobic conditions (100% acetonitrile), indicating that interstrand cross-linked products are not formed. At reaction times above 12 h, multiple low molecular weight species, eluting at low retention times, appear gradually in the HPLC profile. These species most likely arise from depurination of the oligonucleotide under the acidic conditions employed and typically comprise 17–25% of the total UV absorbance area in the elution profile by the end of the reaction. As a result, reactions were usually halted by freezing before the monofunctional intermediates had been converted completely to the bifunctional product in order to minimize the loss by decomposition. The bifunctional adduct typically comprised ~40% of the total UV absorbance area at the end of the reaction, while monoadducts comprised 20% and unreacted dodecamer 10%. The yield of the bifunctional adduct after HPLC purification was typically 23–28%.

Characterization of the Bifunctional Adduct. The predominant product of the reaction at pH 3 between *trans*-DDP and d(CCTCGAGTCTCC) was characterized by ^1H NMR spectroscopy. Downfield regions of the 500-MHz ^1H NMR spectra of platinated and unplatinated single-stranded dode-

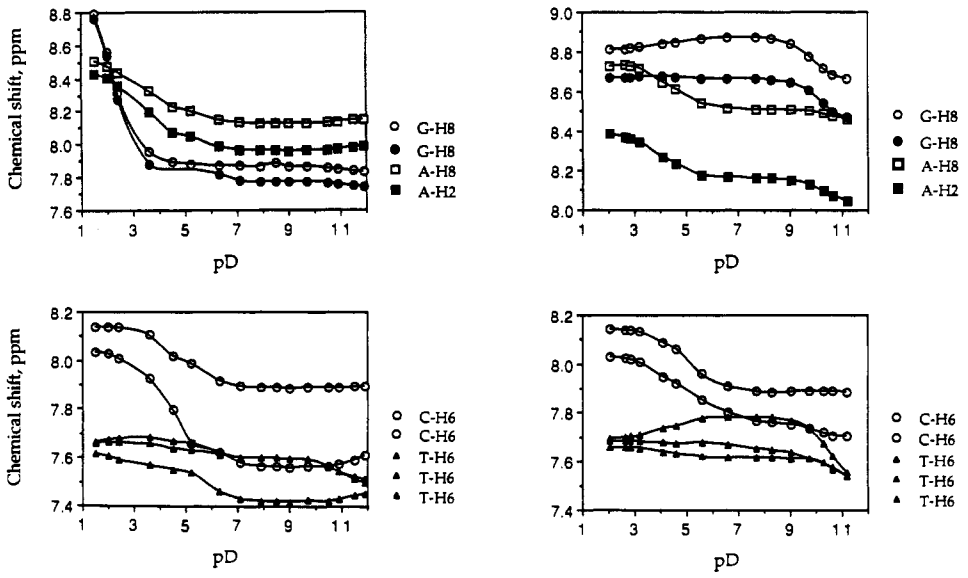

FIGURE 2: Chemical shifts of the nonexchangeable base protons of (left) d(CCTCGAGTCTCC) and (right) *trans*-[$Pt(NH_3)_2$\{d(CCTCGAGTCTCC)\}] at 35 °C as a function of pD. Purine H8 and H2 resonances are shown at the top and pyrimidine H6 resonances at the bottom. The cytosine H6 curves represent positions of the farthest upfield and downfield resonances in the overlapping set of H6 doublets.

camer are shown in Figure S1 of the supplementary material.

Nonexchangeable base proton resonances were assigned primarily on the basis of pD-dependent chemical shift studies, as shown in Figure 2. The plots exhibit characteristic sigmoidal shapes with midpoints corresponding to pK_a values of the nucleobase endocyclic N–H groups (Izatt et al., 1971; Saenger, 1984). For the unplatinated dodecamer, H8 singlets of G(5) and G(7) are assigned on the basis of their positions downfield of the pyrimidines, protonation at N7 with $pK_a \approx 2$, and deprotonation of N1 at or above pD 10.4. The H8 (downfield) and H2 (upfield) resonances of A(6) are identified by their downfield positions, the fact that they shift in concert throughout the pD titration, and the characteristic protonation at N1 $\approx$ pD 3. Cytosine H6 resonances were not resolved throughout the entire pD range, so Figure 2 shows the positions of the most upfield and downfield resonances in the envelope. Cytosine H6 resonances are readily identified by their characteristic doublet structure ($^3J_{H5-H6} = 7$ Hz) as well as protonation of N3 between pD 4 and 4.5. Thymidine H6 singlets are assigned on the basis of their characteristic upfield positions and the onset of N3 deprotonation near pD 10.

For the platinated dodecamer, the purine resonances exhibit pronounced downfield shifts relative to their positions in the unplatinated single strand. The guanosine H8 resonances exhibit the largest shifts, a phenomenon well-known to accompany *cis*- (Inagaki & Kidani, 1979; Caradonna & Lippard, 1988; van der Veer at al., 1986) and *trans*-DDP (van der Veer et al., 1986; Gibson & Lippard, 1987; Lepre et al., 1987) binding to DNA. The lack of N7 protonation near pD 2 and the observed decrease by at least 1.1 units in the pK_a of N1 to 9.3 indicate platinum binding to N7 positions of both G(5) and G(7) (van der Veer et al., 1986; Gibson & Lippard, 1987; Lepre et al., 1987). From AAS and UV spectroscopy, there is one bound platinum atom per strand. Thus, *trans*-$\{Pt(NH_3)_2\}^{2+}$ is bifunctionally coordinated, forming a 1,3-intrastrand cross-link between the guanosine N7 positions. This assignment is corroborated by enzymatic digestion analysis (vide infra). As in the unplatinated dodecamer, the remaining adenosine H8 and H2 resonances shift upon protonation at N1 ($pK_a = 3.8$), as do the cytosine H6 doublets upon protonation of N3 ($pK_a = 4.6$) and the thymidine H6 singlets upon the onset of N3 deprotonation near pD 10.

Resonances of the central adenosine in the platinated single-stranded dodecamer exhibit the same downfield shifts ($\Delta\delta = 0.2$ and 0.4 ppm) as observed for the central bases of other *trans*-DDP 1,3-intrastrand cross-links (van der Veer et al., 1986; Gibson & Lippard, 1987; Lepre et al., 1987). We therefore conclude that A(6) is similarly destacked from its neighboring bases.

Identification of Monofunctional Adducts. Monofunctionally bound intermediates formed during the reaction of *trans*-DDP with d(CCTCGAGTCTCC) were identified by trapping them as triammineplatinum(II) monoadducts (Fichtinger-Schepman et al., 1984, 1988a). Addition of $NH_4(HCO_3)$ to the reaction mixture after 4 h halted the platination reaction, producing two major and one minor products that eluted with retention times identical with those obtained by reaction of $[Pt(NH_3)_3Cl]^+$ with the dodecamer. The fact that the intermediates react with NH_4^+ and thiourea (vide infra) indicates the presence of an open Pt coordination site and hence monofunctional binding.

Under mild conditions, thiourea rapidly reacts with *trans*-DDP monofunctional adducts and labilizes them from DNA, presumably due to the trans labilizing effect of the sulfur ligand (Eastman & Barry, 1987). Intermediates formed during the reaction of *trans*-DDP with d(CCTCGAGTCTCC) were allowed to react with a 50-fold excess of thiourea in order to determine if they would similarly be trapped and removed. The addition of thiourea after 4 h immediately halted the platination reaction, and after an additional 10 min of reaction at room temperature the concentration of monofunctional adducts had decreased by roughly 90% (supplementary material, Figure S2). Extended reaction with thiourea resulted in complete removal of monoadducts, as evidenced by reappearance of the unmodified dodecamer; a fraction of the platinum remained as bifunctional adducts. Incubation of triammine monoadducts formed on the dodecamer by $[Pt(NH_3)_3Cl]Cl$ with 50 mM thiourea for 50 min at 37 °C gave no apparent reaction. This result is expected since these monoadducts do not possess a substitutionally labile site.

Since the reaction of $[Pt(NH_3)_3Cl]Cl$ with d(CCTCGAGTCTCC) gave the same products as the $NH_4(HCO_3)$ trapping reaction, with no loss of platinum due to formation of bifunctional adducts or decomposition during the course of incubation at pH 8, the reaction of $[Pt(NH_3)_3Cl]Cl$ with the dodecamer was used to generate sufficient quantities of the two major monoadducts for further study. The two major monoadducts, henceforth referred to as M1 and M2, were purified by HPLC and characterized. It was not possible to isolate sufficient quantities of the minor monoadduct for further characterization.

The sites of platinum binding in the two major monoadducts (M1, M2) and the bifunctional adduct (B1) were determined by enzymatic digestion analysis, as shown in Figure 3. The digestion process does not disrupt Pt–DNA bonds (Fichtinger-Schepman et al., 1982). HPLC elution profiles of the digestion mixtures contain peaks arising from the unmodified 2′-deoxynucleosides as well as traces of impurities from the digestion matrix or incompletely dephosphorylated species that elute in the column void volume. In the case of B1, a small peak eluting between dT and dA probably corresponds to incompletely digested *trans*-$[Pt(NH_3)_2(dG)\{d(GpN)\}]^{2+}$ (N = A or T) (Eastman et al., 1988). The relative intensity ratios of the 2′-deoxynucleoside peaks for all samples were in reasonably good agreement with expected values. The 2′-deoxyguanosine peak is almost absent from the HPLC elution profile of the digestion mixture of B1, and a new peak appears that elutes midway between dC and dG. This peak coelutes with independently synthesized *trans*-$[Pt(NH_3)_2(dG\text{-}N7)_2]^{2+}$ and has a relative area roughly equal to that of two 2′-deoxyguanosines, as expected for a G(5)-N7, G(7)-N7 adduct. The 2′-deoxyguanosine peak in the HPLC elution profiles of digestion mixtures of both triammine monoadducts is half as intense as in unmodified dodecamer, and a new peak appears that elutes just after dC. This peak coelutes with $[Pt(NH_3)_3(dG\text{-}N7)]^{2+}$ and has a relative area roughly equal to that of the dG peak, as expected for a dodecamer strand having one $[Pt(NH_3)_3]^{2+}$ bound at either G(5)-N7 or G(7)-N7. The ratios of bound platinum per strand in M1 and M2 are 0.7 ± 0.3 and 0.7 ± 0.2, respectively. Since triammine monoadducts appear as homogeneous peaks in the HPLC elution profile, we conclude that one species corresponds to the G(5)-N7 and the other to the G(7)-N7 adduct. Our experiments do not permit assignment of M1 and M2 to N7 sites of specific guanosines, however. The observation that monofunctional intermediates formed by *trans*-DDP are bound primarily at guanosine N7 positions is consistent with previously determined monofunctional binding preferences of *cis*- and *trans*-DDP, as measured by ammonia trapping (Fichtinger-Schepman et al., 1982, 1985), thiourea trapping (Eastman, 1986, 1987),

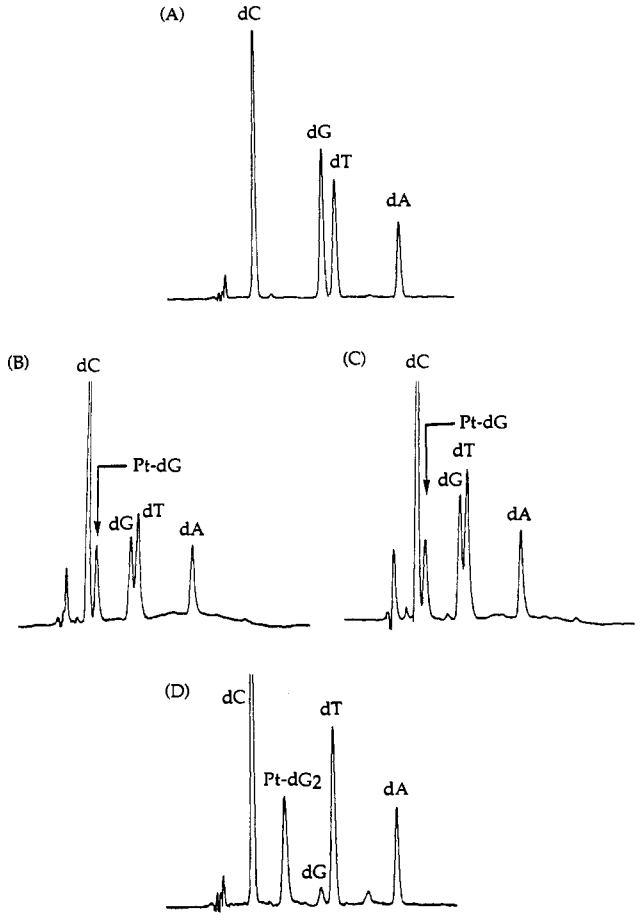

FIGURE 3: Reversed-phase HPLC elution profiles of enzymatically digested unmodified dodecamer, monofunctional adducts, and bifunctional adducts. Peak identities were confirmed by coinjection with standard compounds. The peak labels are as follows: dC, 2′-deoxycytosine (this peak is off-scale); Pt-dG, $[Pt(NH_3)_3(dG\text{-}N7)]^{2+}$; Pt-$dG_2$, *trans*-$[Pt(NH_3)_2(dG\text{-}N7)_2]^{2+}$; dG, 2′-deoxyguanosine; dT, 2′-deoxythymidine; dA, 2′-deoxyadenosine. (A) Products from the digestion of unplatinated d(CCTCGAGTCTCC). (B) Products from the digestion of monoadduct M1. (C) Products from the digestion of monoadduct M2. (D) Products from the digestion of the bifunctional adduct B1 (see Figure 1).

and the mapping of $\{Pt(dien)\}^{2+}$ binding sites (Johnson et al., 1982).

UV Spectroscopic Melting Behavior. The UV melting profiles of the unplatinated and platinated duplexes are shown in Figure 4. Melting temperatures, T_m, were taken from the midpoint of the cooperative portion of the melting curve or from the maximum of the plot of dA_{262}/dT vs T. The absorption maximum occurred at 262 nm for both duplexes and did not shift during the melting transition.

The melting profile of the unplatinated duplex shows a gradual, noncooperative increase in absorbance up to 45 °C, most likely due to differential melting of the terminal base pairs (Borer et al., 1975; Patel & Hilbers, 1975; Patel, 1978; Pardi et al., 1981; Kan et al., 1982; Patel et al., 1982a,b; Caradonna & Lippard, 1988), followed by a sharp, cooperative increase between 45 and 55 °C with a midpoint T_m at 48 °C. The platinated duplex has a similar melting profile. The absorbance increases noncooperatively up to 45 °C, followed by a cooperative increase having a midpoint T_m at 52 °C. There is little increase in the absorbance above 55 °C for either duplex. Since initial melting of the duplexes was noncooperative, the oligonucleotides exist in more than two states, and no attempt was made to calculate thermodynamic parameters from the melting curves.

Temperature Dependence of the Exchangeable Base Proton Resonances. UV melting profiles of oligonucleotide duplexes provide a measure of their thermal stability, but a more detailed assessment of melting can be obtained from NMR spectroscopy, where the behavior of individual base pairs can be observed. It was unfortunately not possible completely to resolve and assign nonexchangeable base or sugar proton resonances of either the platinated or unplatinated duplexes. Although the unplatinated duplex spectra were better resolved, they were not analyzed in detail since our interest was in the platinated form. The resonances of the platinated duplex were especially broadened owing to sample aggregation at the concentrations necessary for NMR spectroscopic studies. This aggregation parallels that reported for other short oligonucleotide duplexes and is more pronounced for platinated DNA and in high salt (Fried & Bloomfield, 1984; Härd &

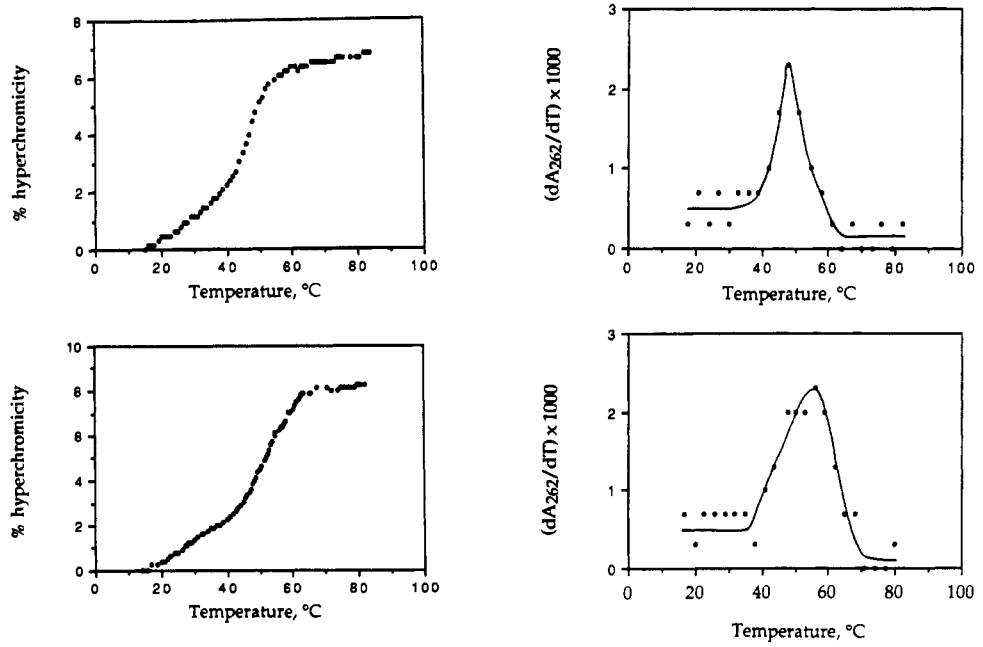

FIGURE 4: UV absorbance melting curves and first derivative plots for unmodified (top) and *trans*-$\{Pt(NH_3)_2\}^{2+}$-modified (bottom) dodecanucleotide duplexes, in 0.1 M potassium phosphate buffer at pH 7.

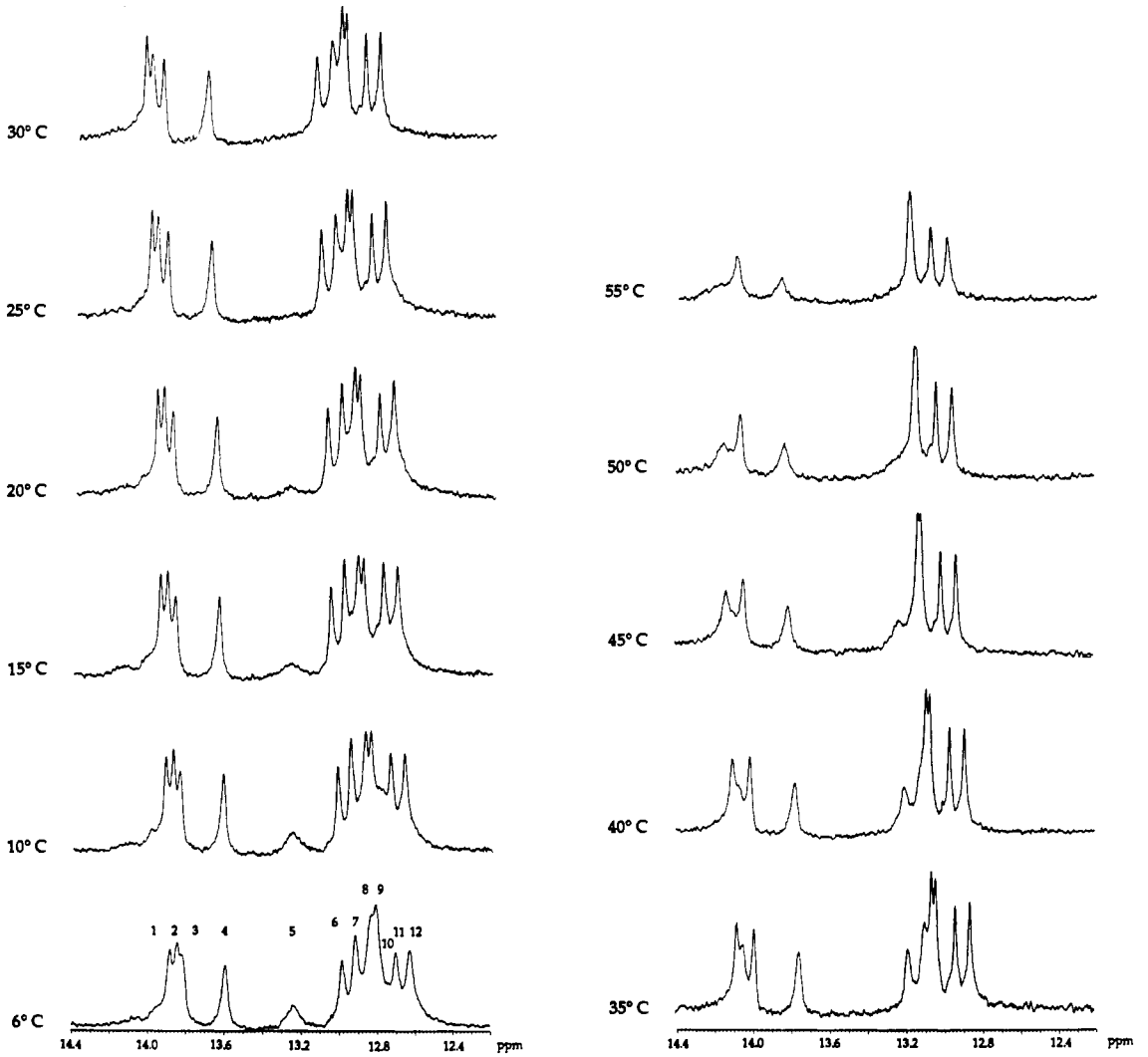

FIGURE 5: Temperature dependence of the imino proton resonances of d(CCTCGAGTCTCC)·d(GGAGACTCGAGG), 1 mM duplex in 90% H_2O, 10% D_2O, and 0.1 M NaCl at pH 7.

Kearns, 1986; Lepre et al., 1987; Caradonna & Lippard, 1988). Pronounced broadening of the ^1H NMR spectrum has also been reported recently for the duplex form of *cis*-[Pt-$(NH_3)_2$[d(TTTTCGCGTTTT)-*N7-G(6),N7-G(8)*] (Ptak et al., 1989). Aggregation of oligonucleotides may be facilitated by platination with $\{Pt(NH_3)_2\}^{2+}$, owing to partial charge neutralization, local base destacking, and the formation of interduplex hydrogen bonds by the ammine ligands.

The exchangeable amino NH resonances overlapped with nonexchangeable base proton resonances and could not be resolved, but the less numerous exchangeable imino (G-N1 and T-N3) proton resonances appeared in a relatively uncrowded downfield region of the spectrum, permitting their resolution. Accordingly, a comparative study of the temperature dependence of the imino proton resonances of the unplatinated and platinated duplexes was carried out, providing useful information regarding the rates of proton exchange from the duplex.

The temperature dependence of the imino proton resonances of the unplatinated duplex is shown in Figure 5. All 12 imino proton resonances are observed at 6 °C, and their shifts are listed in Table I. The resonances could not be accurately integrated because the binomial pulse sequence produces a nonuniform excitation pattern over the width of the spectrum (Hore, 1983). Four thymine N3 proton resonances appear in the downfield region, characteristic of A·T base pairs, and seven individual guanine N1 proton resonances occur in the upfield region, as expected for G·C base pairs (Patel & Canuel, 1979; Hilbers, 1979; Gorenstein, 1984; Wüthrich, 1986). The broad, overlapping peak (resonance 10 in Figure 5) is tentatively assigned to the remaining guanine N1 proton resonances. No resonances occurred in the 10–12 ppm region, where protons in mismatched, looped, or non-base-paired structures would characteristically appear. Exchange and dissociation

Table I: Chemical Shifts and Melting Behavior of the Imino Proton Resonances of d(CCTCGAGTCTCC)·d(GGAGACTCGAGG) in 0.1 M NaCl

resonance peak	chemical shift at 10 °C, δ (ppm)	range of broadening (°C)	
		onset	completion
	A·T Resonances		
1	13.86	40	60
2	13.82	20	55
3	13.79	50	65
4	13.56	45	65
	G·C Resonances		
5	13.19	≤6	25
6	12.96	30	50
7	12.89	20	50
8	12.82	50	≥65
9	12.79	50	≥65
10[a]	~12.73	≤6	~20
11	12.68	50	≥65
12	12.61	50	≥65

[a] Not resolved.

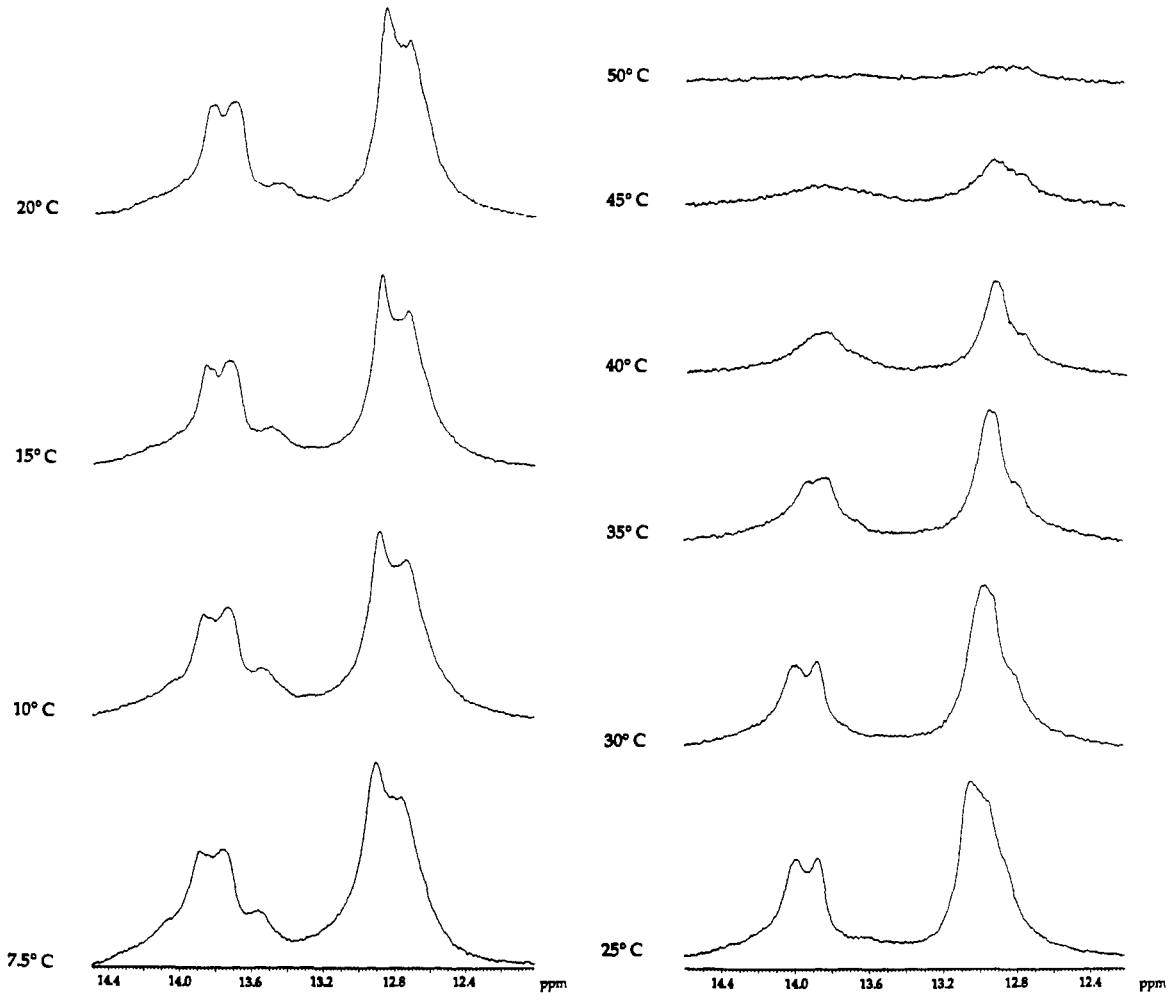

FIGURE 6: Temperature dependence of the imino proton resonances of *trans*-[$Pt(NH_3)_2$[d(CCTCGAGTCTCC)·d(GGAGACTCGAGG)-*N7-G(5),N7-G(7)*]], 1 mM in 90% H_2O, 10% D_2O, and 0.1 M NaCl at pH 7.

rates for individual base pairs could not be measured owing to overlap of imino resonances.

As the temperature is increased, the imino proton resonances broaden and disappear due to rapid exchange with solvent. Two G·C proton resonances (5 and 10 in Figure 5) are partially broadened even at 6 °C and disappear by 25 °C due to rapid exchange with solvent. Although assignments of imino resonances to specific base pairs could not be made, the rapid exchange behavior of these resonances indicates that they arise from the terminal base pairs, C(1)·G(24) and C(12)·G(13), which are expected to undergo kinetic "fraying" even at low temperatures (Borer et al., 1975; Kan et al., 1975; Patel, 1978; Patel et al., 1982a,b; Fritzsche et al., 1983). G·C base pair resonances 6 and 7 begin to broaden at 20 °C and are in rapid exchange by 50 °C, indicating that they most likely correspond to frayed base pairs C(2)·G(23) and C(11)·G(14) near the termini, consistent with the common tendency of short oligonucleotide duplexes to fray and melt sequentially inward from the ends (Borer et al., 1975; Patel & Hilbers, 1975; Patel, 1978; Pardi et al., 1981; Patel et al., 1982a,b; Fazakerly et al., 1985; Rinkel et al., 1987a,b). A·T base pair resonances 1 and 2 exchange in 20–55 °C and 40–60 °C ranges, respectively. This behavior is assigned to sequential exchange of base pairs T(3)·A(22) and T(10)·A(15). The remaining A·T base pairs, resonances 3 and 4, begin to undergo exchange broadening at 45–50 °C and are in rapid exchange with solvent by 65 °C, slightly below the exchange temperature of the remaining G·C resonances. The central A(6)·T(19) and T(8)·A(17) base pairs are therefore capable of undergoing rapid exchange at a temperature at which the central G·C base pairs are still relatively intact. G·C resonances 8, 9, 11, and 12 are the last imino resonances to exchange out, and they all broaden and disappear simultaneously in a narrow range between 55 and 65 °C. This cooperative transition is consistent with the melting of a stable, central core of G·C base pairs, most likely C(4)·G(21), G(5)·C(20), G(7)·C(18), and C(9)·G(16).

The temperature dependence of the imino proton resonances of the platinated duplex is shown in Figure 6. The resonances are broader than for the unplatinated duplex, perhaps owing to greater sample aggregation. The possibility that this broadening is due to solvent viscosity effects is precluded by the sharp appearance of the internal reference peak (not shown) in all spectra. The observation of imino resonances indicates that the platinated oligonucleotide forms a duplex with its complementary strand. The assignment of the imino resonances by base pair type is necessarily uncertain, owing to the unknown effects of platinum binding upon their chemical shifts. No resonances are observed in the 10–12 ppm region. At 7.5 °C, three to four resonances appear in the downfield region where A·T base pair resonances normally occur. If all these resonances arise from A·T base pairs, then the central A(6)·T(19) base pair would have to be intact, a possibility considered unlikely on the basis of the tendency of the central adenosine base to destack in the single-stranded adduct (vide supra). Possibly one or more of these downfield resonances correspond to G·C base pairs that are deshielded relative to their positions in the unplatinated duplex. Four to six reso-

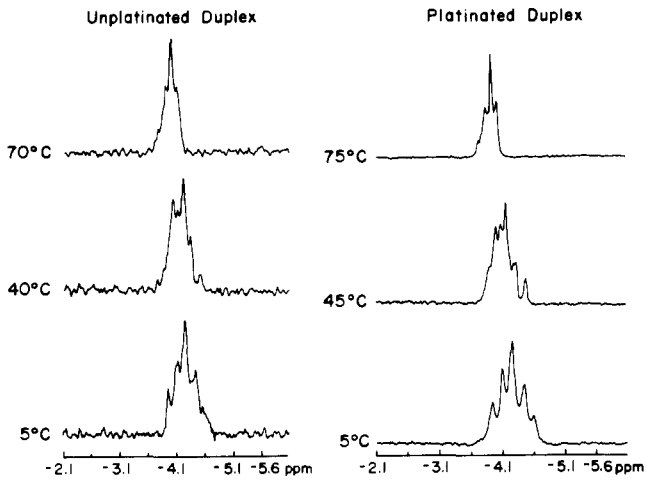

FIGURE 7: Temperature-dependent ^{31}P NMR spectra of (left) unplatinated and (right) platinated oligonucleotide duplexes, under the same conditions as Figure 5. Shifts are referenced to internal trimethyl phosphate.

nances are observed in the G·C base pair region of the spectrum at 7.5 °C. The absence of several guanine imino resonances is consistent with increased accessibility of the G(5) and G(7) imino protons induced by *trans*-$\{Pt(NH_3)_2\}^{2+}$ binding at their N7 positions. Two of the resonances in the A·T base pair region are broad even at 7.5 °C and are in rapid exchange by 30 °C, while the remaining two begin to broaden at 30 °C and are in rapid exchange by 50 °C; all exhibit gradual, rather than cooperative, changes in line width. Resonances in the G·C base pair region consist of several overlapping peaks. These resonances exhibit small, upfield chemical shift changes beginning at 25 °C and broaden out over a larger range (25–50 °C) than the G·C core imino resonances of the unplatinated duplex (55–65 °C).

These results thus reveal that the unplatinated duplex is fully base paired at low temperatures, exhibiting imino proton exchange behavior consistent with that expected of a short oligonucleotide duplex. Melting presumably begins with noncooperative, successive duplex disruption from the terminal base pairs inward. Imino protons of the inner A·T base pairs exchange more rapidly than the neighboring G·C base pairs without disrupting them. Finally, the remaining G·C base pairs exchange out simultaneously over a narrow temperature range, as expected if the duplex does not fully melt until the T_m of the high-melting G·C core is reached, at which point they melt cooperatively. Although the platinated dodecamer can form a duplex, platinum binding causes at least two of the G·C base pairs to undergo rapid exchange with solvent at 7.5 °C. The imino protons of the G·C core undergo rapid exchange at a temperature approximately 15 °C lower than observed for the unplatinated duplex, indicating that platination of the N7 positions of G(5) and G(7) facilitates the exchange of the base pairs in the central portion of the duplex.

Temperature-Dependent ^{31}P NMR Spectroscopy. Temperature-dependent ^{31}P NMR spectra of the unplatinated and platinated duplexes are shown in Figure 7. It was not possible to assign resonances from the available information. Allowing for differences due to the number of transients acquired, the spectra for both duplexes are virtually identical at all temperatures, showing an overlapping pattern of resonances centered about −4.25 ppm. This pattern indicates a range of phosphate conformations consistent with a predominantly A- or B-DNA structure, with some local structural heterogeneity. There is no evidence of downfield-shifted resonances corresponding to Z-DNA (Gorenstein, 1984), bulged structures

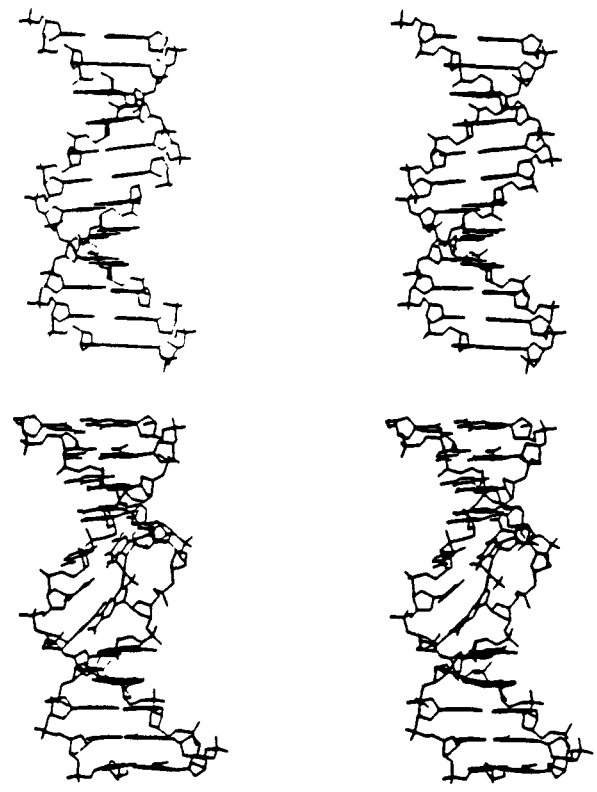

FIGURE 8: Stereoview comparing dodecanucleotide duplex models. Top, B-DNA structure of d(CCTCGAGTCTCC)·d(GGAGACTCGAGG); bottom, molecular dynamics model structure of *trans*-$[Pt(NH_3)_2\{d(CCTCGAGTCTCC)\cdot d(GGAGACTCGAGG)$-*N7-G(5),N7-G(7)*$\}]$.

(Patel et al., 1982c; Roy et al., 1987), or terminal phosphates (Bower et al., 1987). There is also no evidence of a phosphate resonance near −3.0 ppm, known to arise from reduction of the O–P–O angle of the central phosphate of a *cis*-$[Pt(NH_3)_3\{d(GpG)$-*N7,N7*$\}]$ chelate in DNA (Wilson et al., 1982; den Hartog et al., 1984; Marzilli et al., 1984) and duplex oligonucleotides (Marzilli et al., 1984; den Hartog et al., 1984, 1985; Reily & Marzilli, 1985; Fouts et al., 1987). Hydrogen bonding of the central phosphate to ammine ligands on the platinum center also contributes to this downfield shift (Fouts et al., 1987, 1988). Our results are in agreement with previously reported spectra of adducts formed by *trans*-DDP and [Pt(dien)Cl]Cl on DNA (Marzilli et al., 1984; Reily & Marzilli, 1985) and oligonucleotides (Fouts et al., 1987), in which downfield-shifted ^{31}P resonances were not observed.

The spectra undergo only slight changes between 5 and 40 °C. Between 40 and 70 °C, there are sharp downfield shifts of equal magnitude (0.1–0.4 ppm) for both duplexes, and the envelope of resonances collapses from a pattern spanning a chemical shift range of 0.63–0.66 ppm to a narrow set that is 0.34–0.35 ppm wide. A plot of chemical shift of the central resonance of the platinated duplex versus temperature (Figure S3, supplementary material), behavior representative of all resonances, shows that the cooperative 0.2 ppm downfield shift has a midpoint of 55–65 °C. This transition is the same (midpoint within 5 °C) as observed for the unplatinated duplex and occurs at a temperature where the imino resonances of the duplex all undergo rapid exchange with solvent. The cooperative transition observed by ^{31}P NMR spectroscopy is probably the same type as followed by UV spectroscopy but occurs at a higher temperature because of the higher oligonucleotide concentration employed for the NMR studies.

Molecular Modeling. Stereoviews comparing the platinated duplex model with a B-DNA model structure for the unpla-

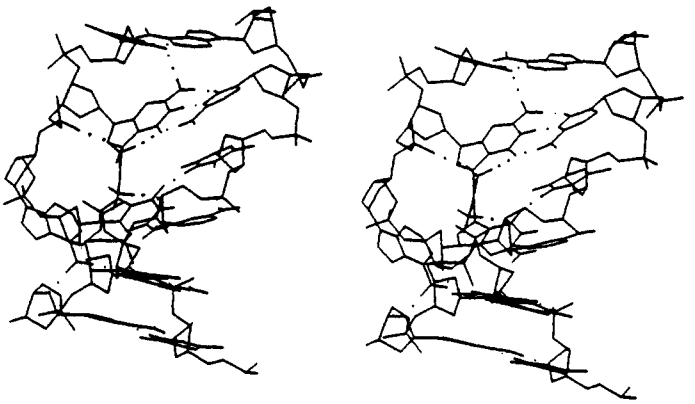

FIGURE 9: Stereoview showing the central portion of the molecular dynamics model structure of *trans*-[Pt(NH$_3$)$_2$[d(CCTCGAGTCTCC)·d(GGAGACTCGAGG)-*N7-G(5),N7-G(7)*}]. Hydrogen bonds between bases are depicted with dotted lines.

Table II: Structural Details of the Central Portion of the Model Structure of *trans*-[Pt(NH$_3$)$_2$[d(CCTCGAGTCTCC)·d(GGAGACTCGAGG)-*N7-G(5),N7-G(7)*}]

bonds	distance (Å)
Pt-N7[G(5)]	2.02
Pt-N7[G(7)]	2.00
Pt-N[NH$_3$(A)]	2.02
Pt-N[NH$_3$(B)]	2.01
nonbonded or H-bonded contacts	**distance (Å)**
NH$_3$(A)-O[G(7)-5′-PO$_4$]	3.12
NH$_3$(A)-O6[G(7)]	3.02
NH$_3$(B)-O4′[C(20)]	3.02
O6[G(5)]-N1[T(19)]	3.28
O4′[G(5)]-N2[G(21)]	2.78
O6[G(7)]-N4[C(18)]	2.85
N6[A(6)]-N3[G(21)]	2.65
N6[A(6)]-O4′[A(22)]	2.66
N2[G(7)]-O2[C(18)]	2.61
N3[G(7)]-N1[C(18)]	2.78
N2[G(7)]-O2[T(8)]	2.70

tinated duplex appear in Figure 8. Four bases at the 5′ end and five at the 3′ end of the platinated model duplex are fully paired and retain B-DNA type conformations. The two N7-coordinated guanine bases tilt off the stack, increasing the interplanar angles between C(4) and G(5) and between G(7) and T(8) to 50.4° and 58°, respectively, and causing the N9-C1′-C5-C8 improper angles to deviate by 15° from planarity. The central A(6) base destacks from its neighbors and lies in the minor groove. Its sugar adopts an N conformation, allowing the backbone to contract by decreasing the distance between the G(5) and G(7) phosphates from 12.3 to 10 Å. The other sugar rings retain S conformations.

The base pairing and stacking of the central portion of the platinated model duplex are shown in more detail in Figure 9. Binding of the *trans*-{Pt(NH$_3$)$_2$}$^{2+}$ moiety in the model duplex completely disrupts the G(5)·C(20) base pair, causing C(20) to rotate in order to stack with G(21) and T(19). The G(7)·C(18) base pair remains essentially intact, with C(18) rotating in order to maintain base pairing, resulting in a C(18)-A(17) interplanar angle of 39.4°. In addition, as listed in Table II, the amino group of G(7) forms a bifurcated hydrogen bond with O2 of T(8). The central A(6) in the minor groove forms two hydrogen bonds, between its amino group and O4′ of A(22) and N3 of G(21). The ammines coordinated to platinum form hydrogen bonds that bridge the two strands, with one ammine bonding to the O4′ of C(20) and the other bonding to both the 5′-phosphate oxygen and O6 of G(7).

The model for the platinated oligonucleotide duplex exhibits a bend induced by formation of the 1,3-intrastrand chelate. Unlike molecular mechanics models for the 1,2-GpG intrastrand adduct of *cis*-DDP on a duplex, which exhibit a kink of between 40° and 70° in the direction of the major groove (Miller et al., 1985; Kozelka et al., 1985, 1986, 1987), the model for the *trans*-DDP 1,3-intrastrand adduct on a duplex bends in the direction of the vector connecting the C1′ atoms of A(6) and T(19). The magnitude of the kink is 18°, as measured from the angle subtended by the helix axes of the unperturbed terminal base pairs of the duplex. A view comparing kinks of *cis*- and *trans*-DDP adduct models is provided in Figure S4 (supplementary material). Binding of *trans*-DDP to G(5) and G(7) appears to induce bending by causing the backbone to contract, shifting the bases in the 5′-direction; the duplex must bend in order to preserve the base pairing.

Discussion

The reaction of *trans*-DDP with d(CCTCGAGTCTCC) proceeds through formation of monofunctional intermediates. Two predominant intermediates form rapidly, each having one *trans*-{Pt(NH$_3$)$_2$X}^{n} (X is a labile group, Cl- or H$_2$O) moiety bound at N7 of G(5) or G(7); a third intermediate is formed more slowly. The preference of *trans*-DDP to bind initially at guanosine N7 positions is consistent with studies of other investigators, most notably results for the reaction of *trans*-DDP with single-stranded salmon sperm DNA (Eastman et al., 1988). The identity of the third intermediate is not known, but it could correspond to a monofunctional adduct at A(6). Such a species would form more slowly due to protonation at N1, or due to the lower propensity of platinum to bind to adenosine compared to guanosine (Mansy et al., 1978). Alternatively, the third intermediate could have two platinum atoms bound at, for example, N7 positions of both guanosines, or at the N1 and N7 positions of the same or different bases. It is not obvious why the concentration of such a species would subsequently decline, however.

The appearance and disappearance of monofunctional adducts have a time dependence characteristic of two consecutive first-order reactions affording a single product. The consumption of d(CCTCGAGTCTCC) follows pseudo-first-order kinetics. The rate constant of $(12.5 \pm 0.4) \times 10^{-5}$ s^{-1} is comparable to the value of $(9.6 \pm 0.4) \times 10^{-5}$ s^{-1} measured for reaction of *trans*-DDP with DNA by ^{195}Pt NMR spectroscopy (C. A. Lepre, D. P. Bancroft, and S. J. Lippard, unpublished results), to the value of $(5.4 \pm 0.9) \times 10^{-5}$ s^{-1} measured for binding of *trans*-DDP to DNA by AAS (Ushay et al., 1981), and to the value of $k = 9.8 \times 10^{-5}$ s^{-1} measured for hydrolysis of the first chloride of *trans*-DDP in water (Aprile & Martin, 1962). The data are consistent with *trans*-DDP binding to d(CCTCGAGTCTCC) in two pseudo-first-order steps, the first being the hydrolysis-limited

formation of monofunctional adducts, and the second being closure of the monoadducts to form a bifunctional adduct at the N7 positions of G(5) and G(7).

The *trans*-{$Pt(NH_3)_2$}$^{2+}$-modified oligonucleotide is capable of forming a duplex with its complementary strand, and the melting temperatures of the unplatinated and platinated duplexes are similar. This result is surprising, since studies with oligonucleotide duplexes have shown that the binding of *cis*-DDP to form 1,2- (den Hartog et al., 1984, 1985; van Hemelryck et al., 1984, 1986) and 1,3-intrastrand (den Hartog et al., 1985) adducts dramatically lowers the melting temperature of the duplex. It is, however, consistent with reports that, at low r_b values, *trans*-DDP binding to DNA slightly increases its stability (Macquet & Butour, 1978; Vrâna et al., 1986). The similarity between the ^{31}P NMR spectra of the unplatinated and platinated duplexes, moreover, indicates that *trans*-DDP does not induce large changes in the phosphate backbone of the duplex.

The imino proton resonances of several G·C base pairs are absent from the ^1H NMR spectrum of the platinated duplex, even at 7.5 °C, and all of the imino protons of the platinated duplex undergo rapid exchange with solvent by 50 °C, at which temperature the oligonucleotide is roughly 50% double stranded. This result indicates that the imino protons of the platinated duplex are inherently more accessible for exchange with solvent and that the average lifetimes of all imino protons are short at a temperature where the actual fraction of dissociated duplex is relatively small.

A molecular dynamics model calculated for the platinated duplex is generally consistent with these experimental results. The *trans*-DDP adduct is accommodated with only localized destacking of bases and minimal distortion of the O–P–O angles, although the dependence of the ^{31}P shifts on both torsion and O–P–O angles precludes prediction of specific resonance positions. The G(5)·C(20) and A(6)·T(19) base pairs are disrupted and, along with adjoining base pairs, are readily available for exchange with solvent. The model thus accounts for the rapid exchange of the imino protons at low temperatures observed experimentally. The G(7)·C(18) base pair is intact, but the experimental evidence is insufficient to confirm this point for the actual duplex. The N conformation of the A(6) sugar in the model differs from results observed for *trans*-DDP 1,3 adducts on single-stranded oligonucleotides, in which only the sugar of the 5′-nucleotide in the chelate adopts an N conformation (van der Veer et al., 1986; Gibson & Lippard, 1987; Lepre et al., 1987). Experimental data available for the platinated duplex studied here do not reveal sugar conformations, but it is possible that structural constraints imposed by base pairing in a double helix may produce different sugar conformations for single- and double-stranded adducts.

The molecular model for the platinated duplex exhibits several features that help to explain its unexpected stability. Hydrogen bonds formed by the platinum ammine ligands in the model would help prevent duplex dissociation while allowing base pair proton exchange. Furthermore, shifting the central adenosine base into the minor groove may help stabilize the duplex, both by the formation of additional hydrogen bonds and by "quasi-intercalation" of the aromatic ring between the walls of the minor groove, as indicated for the DNA binding antibiotic netropsin (Berman et al., 1979; Yoon et al., 1988).

Finally, in addition to being consistent with previously noted ^{31}P NMR spectroscopic and optical melting studies, the conclusion that *trans*-DDP does not significantly destabilize the double helix also concurs with the results of investigations employing other techniques. Assays of the differential cleavage of platinated DNA by single-strand-sensitive S1 nuclease (Mong et al., 1981; Eastman, 1982; Scovell & Capponi, 1982, 1984), as well as experiments that detect denaturation by Tb^{3+} fluorescence (Houssier et al., 1983), indicate that *cis*-DDP binding induces greater disruption of DNA secondary structure than seen for the trans isomer. Interestingly, a study employing antinucleoside antibodies (Sundquist et al., 1986) revealed that, at equivalent levels of bound platinum, antibodies to all four nucleosides reacted more avidly with DNA modified by *trans*- versus *cis*-DDP, indicating that the trans isomer exposes the bases to a greater extent. These results are not inconsistent with the present model in which greater base pair disruption at the site of platination occurs for DNA containing *trans*-DDP adducts, despite the greater overall duplex stability.

In conclusion, the present studies reveal that the *trans*-{$Pt(NH_3)_2$}$^{2+}$ fragment can form a stable 1,3-intrastrand cross-link between two N7 atoms of d(G) nucleosides, one of the major adducts found when *trans*-DDP binds to DNA. The resulting platinated duplex is structurally very different from that obtained when cisplatin modifies DNA and could account for aspects of the different biological processing of adducts formed by the different isomers. Molecular dynamics calculations afford one possible model for stereochemical details of the *trans*-{$Pt(NH_3)_2$}$^{2+}$ duplex adduct that accounts for the unexpected thermal stability.

Acknowledgments

The MIT mass spectrometry facility is supported by NIH Grant RR 00317 (principal investigator, Prof. K. Biemann) from the Biotechnology Resources Branch, Division of Research Resources. We are grateful to Dr. M. Karplus, in whose laboratory the molecular modeling was performed, and to the Engelhard Corp., for a loan of K_2PtCl_6 from which the platinum complexes were prepared.

Supplementary Material Available

Details of the synthesis and characterization of *trans*-[$Pt(NH_3)_2${d(CCTCGAGTCTCC)-*N7-G(5)*,*N7-G(7)*}] and model complexes, *trans*-[$Pt(NH_3)_2${5′-d(GMP)-*N7-G*}$_2$]$^{2-}$, *trans*-[$Pt(NH_3)_2$(dG-*N7*)$_2$]$^{2+}$, [$Pt(NH_3)_3$(dG-*N7*)]$^{2+}$, and [$Pt(NH_3)_3$Cl]Cl; HPLC elution profiles of thiourea reaction with monofunctional adducts of *trans*-DDP with the dodecamer; temperature-dependent ^{31}P NMR spectra; and comparison of duplex bending by *cis*- and *trans*-{$Pt(NH_3)_2$}$^{2+}$ 1,2- and 1,3-intrastrand cross-links (25 pages). Ordering information is given on any current masthead page.

Registry No. d(CCTCGAGTCTCC), 123994-25-2; *trans*-[$Pt(NH_3)_2${d(CCTCGAGTCTCC)-*N7-G(5)*,*N7-G(7)*}], 124041-99-2; *trans*-DDP, 14913-33-8.

References

Aprile, F., & Martin, D. S. (1962) *Inorg. Chem. 1*, 1373.
Arnott, S., Campbell-Smith, P., & Chandresekharan, P. (1976) in *CRC Handb. Biochem. 2*, 411.
Berman, H. M., Neidle, S., Zimmer, Ch., & Thrum, H. (1979) *Biochim. Biophys. Acta 561*, 124.
Borer, P. N., Kan, L.-S., & Ts'o, P. O. (1975) *Biochemistry 14*, 4847.
Bower, M., Summers, M. F., Kell, B., Hoskins, J., Zon, G., & Wilson, W. D. (1987) *Nucleic Acids Res. 15*, 3531.
Caradonna, J. C., & Lippard, S. J. (1988) *Inorg. Chem. 27*, 1454.
Ciccarelli, R. B., Solomon, M. J., Varshavsky, A., & Lippard, S. J. (1985) *Biochemistry 24*, 7533.

Clore, G. M., & Gronenborn, A. M. (1982) *J. Am. Chem. Soc. 104*, 1369.
Cohen, G. L., Ledner, J. A., Bauer, W. R., Ushay, H. M., Caravana, C., & Lippard, S. J. (1980) *J. Am. Chem. Soc. 102*, 2487.
den Hartog, J. H., Altona, C., van Boom, J. H., van der Marel, G. A., Haasnoot, C. A., & Reedijk, J. (1984) *J. Am. Chem. Soc. 106*, 1528.
den Hartog, J. H., Altona, C., van den Elst, H., van der Marel, G., & Reedijk, J. (1985) *Inorg. Chem. 24*, 983.
Eastman, A. (1982) *Biochem. Biophys. Res. Commun. 105*, 869.
Eastman, A. (1987) *Pharmacol. Ther. 34*, 155.
Eastman, A., & Barry, M. A. (1987) *Biochemistry 26*, 3303.
Eastman, A., Jennerwein, M. M., & Nagel, D. L. (1988) *Chem.-Biol. Interact. 67*, 71.
Fasman, G. D. (1975) in *Handbook of Biochemistry and Molecular Biology*, 3rd ed., Vol. 1, p 589, CRC Press, Boca Raton, FL.
Fazakerly, G. V., Têoule, R., Guy, A., Fritzsche, H., & Guschlbauer, W. (1985) *Biochemistry 24*, 4540.
Fichtinger-Schepman, A. M., Lohman, P. H., & Reedijk, J. (1982) *Nucleic Acids Res. 10*, 5345.
Fichtinger-Schepman, A. M., van der Veer, J. L., Lohman, P. H., & Reedijk, J. (1984) *J. Inorg. Biochem. 21*, 103.
Fichtinger-Schepman, A. M., van der Veer, J. L., Lohman, P. H., & Reedijk, J. (1985) *Biochemistry 24*, 707.
Fichtinger-Schepman, A. M., Dijt, F. J., De Jong, W. H., van Oosterom, A. T., & Berends, S. F. (1988a) in *Platinum and other metal coordination complexes* in *cancer chemotherapy* (Nicolini, M., Ed.) p 33, Nijhof, Boston.
Fichtinger-Schepman, A. M., Oosteom, A. T., Lohman, P. H., & Berends, S. F. (1988b) *Cancer Res. 48*, 3019.
Fouts, C. S., Reily, M. D., Marzilli, L. G., & Zon, G. (1987) *Inorg. Chim. Acta 137*, 1.
Fouts, C. S., Marzilli, L. G., Byrd, R. A., Summers, M. F., Zon, G., & Shinozuka, K. (1988) *Inorg. Chem. 27*, 366.
Fried, M. G., & Bloomfield, V. A. (1984) *Biopolymers 23*, 2141.
Fritzsche, H., Kan, L.-S., & Ts'o, P. O. (1983) *Biochemistry 22*, 277.
Gibson, D., & Lippard, S. J. (1987) *Inorg. Chem. 26*, 2275.
Gingeras, T., Myers, P., Olson, J., Hanberg, F., & Roberts, R. (1978) *J. Mol. Biol. 118*, 113.
Glasoe, P. K., & Long, F. A. (1960) *J. Phys. Chem. 64*, 188.
Gorenstein, D. G. (1984) *Phosphorus-31 NMR: Principles and Applications*, Academic Press, Orlando; and references cited therein.
Gralla, J. D., Sasse-Dwight, S., & Poljak, L. G. (1987) *Cancer Res. 47*, 5092.
Grotjahn, L., Blöcker, H., & Frank, R. (1985) *Biomed. Mass Spectrom. 12*, 514.
Haasnoot, C. A., & Altona, C. (1979) *Nucleic Acids Res. 6*, 1135.
Härd, T., & Kearns, D. R. (1986) *Biopolymers 25*, 1519.
Harder, H. C., Smith, R. G., & Leroy, A. F. (1976) *Cancer Res. 36*, 3821.
Hemminki, K., & Thilly, W. G. (1988) *Mutat. Res. 202*, 133.
Hilbers, C. W. (1979) in *Biological Applications of Magnetic Resonance* (Shulman, R., Ed.) Academic Press, New York.
Hilbers, C. W., & Patel, D. J. (1975) *Biochemistry 14*, 2656.
Hore, P. J. (1983) *J. Magn. Reson. 54*, 539.
Houssier, C., Maquet, M. N., & Fredericq, E. (1983) *Biochim. Biophys. Acta 739*, 312.
Inagaki, K., & Kidani, Y. (1979) *J. Inorg. Biochem. 11*, 39.
Izatt, R. M., Christensen, J. J., & Rytting, J. H. (1971) *Chem. Rev. 71*, 439.
Johnson, N. P., Macquet, J. P., Wiebers, J. L., & Monsarrat, B. (1982) *Nucleic Acids Res. 10*, 5255.
Kan, L.-S., Borer, P. N., & Ts'o, P. O. (1975) *Biochemistry 14*, 4864.
Kan, L.-S., Cheng, D. M., Jayaraman, K., Leutzinger, E. E., Miller, P. S., & Ts'o, P. O. (1982) *Biochemistry 21*, 6723.
Kozelka, J., Petsko, G. A., Quigley, G. J., & Lippard, S. J. (1985) *J. Am. Chem. Soc. 107*, 4079.
Kozelka, J., Petsko, G. A., Quigley, G. J., & Lippard, S. J. (1986) *Inorg. Chem. 25*, 1075.
Kozelka, J., Archer, S., Petsko, G. A., & Lippard, S. J. (1987) *Biopolymers 26*, 1245.
Lepre, C. A., Strothkamp, K. G., & Lippard, S. J. (1987) *Biochemistry 26*, 5651.
Lippard, S. J. (1987) *Pure Appl. Chem. 59*, 731.
Macquet, J. P., & Butour, J. L. (1978) *Biochimie 60*, 901.
Mansy, S., Chu, G. Y. H., Duncan, R. E., & Tobias, R. S. (1978) *J. Am. Chem. Soc. 100*, 607.
Marzilli, L. G., Reily, M. D., Heyl, B. L., McMurray, C. T., & Wilson, W. D. (1984) *FEBS Lett. 176*, 389.
Miller, K. J., Taylor, E. R., Basch, H., Krauss, M., & Stevens, W. J. (1985) *J. Biomol. Struct. Dyn. 2*, 1157.
Mong, S., Daskal, Y., Prestayko, A. W., & Crooke, S. T. (1981) *Cancer Res. 41*, 4020.
Nilsson, N., & Karplus, M. (1986) *J. Comput. Chem. 7*, 591.
Pardi, A., Martin, F. N., & Tinoco, I. (1981) *Biochemistry 20*, 3986.
Patel, D. J. (1978) *Eur. J. Biochem. 83*, 453.
Patel, D. J., & Hilbers, C. W. (1975) *Biochemistry 14*, 2651.
Patel, D. J., & Canuel, L. L. (1979) *Eur. J. Biochem. 96*, 267.
Patel, D. J., Pardi, A., & Itakura, K. (1982a) *Science 216*, 581.
Patel, D. J., Kozlowski, S. A., Marky, L. A., Broka, C., Rice, J. A., Itakura, K., & Breslauer, K. J. (1982b) *Biochemistry 21*, 428.
Patel, D. J., Kozlowski, S. A., Marky, L. A., Rice, J. A., Borka, C., Itakura, K., & Breslauer, K. J. (1982c) *Biochemistry 21*, 445.
Pinto, A. P., & Lippard, S. J. (1985a) *Biochim. Biophys. Acta 780*, 167.
Pinto, A. P., & Lippard, S. J. (1985b) *Proc. Natl. Acad. Sci. U.S.A. 82*, 4616.
Ptak, M., Rahmouni, A., Mazean, K., Thuong, N. T., & Leng, M. (1989) *Anticancer Drug Des. 4*, 53.
Reedijk, J. (1987) *Pure Appl. Chem. 89*, 181.
Reily, M. D., & Marzilli, L. G. (1985) *J. Am. Chem. Soc. 107*, 4916.
Rinkel, L. J., van der Marel, G. A., van Boom, J. H., & Altona, C. (1987a) *Eur. J. Biochem. 163*, 275.
Rinkel, L. J., van der Marel, G. A., van Boom, J. H., & Altona, C. (1987b) *Eur. J. Biochem. 163*, 287.
Roberts, J. J. (1988) *Pontif. Acad. Sci. Scr. Varia 70*, 464.
Roy, S., Sklenár, V., Appella, E., & Cohen, J. (1987) *Biopolymers 26*, 2041.
Saenger, W. (1984) in *Principles of Nucleic Acid Structure*, p 105, Springer-Verlag, New York.
Scovell, W. M., & Capponi, V. J. (1982) *Biochem. Biophys. Res. Commun. 107*, 1138.
Scovell, W. M., & Capponi, V. J. (1984) *Biochem. Biophys. Res. Commun. 124*, 367.
Sherman, S. E., & Lippard, S. J. (1987) *Chem. Rev. 87*, 1153.

Sinha, N. (1983) *Tetrahedron Lett. 24*, 5348.
Sundquist, W. I., Lippard, S. J., & Stollar, B. D. (1986) *Biochemistry 25*, 1520.
Ushay, H. M., Tullius, T. D., & Lippard, S. J. (1981) *Biochemistry 20*, 3744.
van der Veer, J. L., Ligtvoet, G. J., van den Elst, H., & Reedijk, J. (1986) *J. Am. Chem. Soc. 108*, 3860.
van Hemelryck, B., Guittet, E., Chottard, G., Girault, J. P., Huynh-Dinh, T., Lallemand, J.-Y., Igolen, J., & Chottard, J. C. (1984) *J. Am. Chem. Soc. 106*, 3037.
van Hemelryck, B., Guittet, E., Chottard, G., Girault, J. P., Herman, F., Huynh-Dihn, T., Lallemand, J.-Y., Igolen, J., & Chottard, J. C. (1986) *Biochem. Biophys. Res. Commun. 130*, 758.
Villani, G., Hübscher, U., & Butour, J. L. (1988) *Nucleic Acids Res. 16*, 4407.
Vrâna, O., Brabec, V., & Kleinwächter, V. (1986) *Anticancer Drug Des. 1*, 95.
Wilson, W. D., Heyl, B. L., Reddy, R., & Marzilli, L. G. (1982) *Inorg. Chem. 21*, 2527.
Wüthrich, K. (1986) *NMR of Proteins and Nucleic Acids*, Wiley & Sons, New York; and references cited therein.
Yoon, C., Privé, G. G., Goodsell, D. S., & Dickerson, R. E. (1988) *Proc. Natl. Acad. Sci. U.S.A. 85*, 6332.

Cloning and Characterization of the Human Colipase cDNA[†,‡]

Mark E. Lowe,[*,§] Jerry L. Rosenblum,[§] Patricia McEwen,[∥] and Arnold W. Strauss[§,∥]

Department of Pediatrics and Department of Biochemistry and Molecular Biophysics, Washington University School of Medicine, St. Louis, Missouri 63114

Received July 26, 1989; Revised Manuscript Received September 7, 1989

ABSTRACT: Pancreatic lipase hydrolyzes dietary triglycerides to monoglycerides and fatty acids. In the presence of bile salts, the activity of pancreatic lipase is markedly decreased. The activity can be restored by the addition of colipase, a low molecular weight protein secreted by the pancreas. The action of pancreatic lipase in the gut lumen is dependent upon its interaction with colipase. As a first step in elucidating the molecular events governing the interaction of lipase and colipase with each other and with fatty acids, a cDNA encoding human colipase was isolated from a λgt11 cDNA library with a rabbit polyclonal anti-human colipase antibody. The full-length 525 bp cDNA contained an open reading frame encoding 112 amino acids, including a 17 amino acid signal peptide. The predicted protein sequence contains 100% of the published protein sequence for human colipase determined by chemical methods, but predicts the presence of five additional NH_2-terminal amino acids and four additional COOH-terminal amino acids. Comparison of the predicted protein sequence with the known sequences of colipase from other species reveals regions of extensive identity. In vitro translation of mRNA transcribed from the cDNA gave a protein of the expected molecular size that was processed by pancreatic microsomal membranes. Sequence analysis of the in vitro translation product after processing demonstrated signal peptide cleavage and the presence of a human procolipase, as exists in the pig and horse colipases. DNA blot analysis was consistent with the presence of a single gene for colipase. RNA blot analysis demonstrated tissue-specific expression of colipase mRNA in the pancreas. Thus, we report, for the first time, a cDNA for colipase. The cDNA predicts a human procolipase and suggests that there may also be processing at the COOH-terminus. The regions of identity with colipase from other species will aid in defining the interaction with lipase and lipids through site-specific mutagenesis.

Pancreatic lipase is essential for the intraduodenal conversion of dietary triglycerides to more polar monoglycerides and fatty acids (Borgstrom & Erlanson-Albertsson, 1984). In vitro, pancreatic lipase activity is inhibited by bile salts. The activity is restored by the addition of another pancreatic protein, colipase, to the reaction. Studies on patients with steatorrhea suggest that the degree of fat malabsorption is proportional to the colipase concentration in the pancreatic juices (Gaskin et al., 1984). The combination of this observation and the marked effect of colipase on lipase activity in vitro suggests that colipase is essential for pancreatic lipase activity under physiological conditions.

The molecular events of colipase interaction with pancreatic lipase have not been elucidated. Colipase binds to pancreatic lipase in the presence or absence of lipids (Erlanson-Albertsson, 1980; Sternby & Erlansson-Albertsson, 1982) and, also, binds to interfaces such as lipid micelles (Borgstrom, 1976). The amino acids involved in the properties have not been identified. Various studies, relying on spectral methods or chemical modification, have implicated amino acids or regions that may be important in these properties of colipase (Borgstrom & Erlanson-Albertsson, 1984). Both types of studies may be monitoring the effects of a conformational change in the protein on the residues that are modified or followed spectrophotometrically. Site-specific mutagenesis affords the opportunity to obtain detailed information about the rela-

[†] This work was supported by NIH Grant DK33487A.
[‡] The nucleic acid sequence in this paper has been submitted to GenBank under Accession Number J02883.
[*] Address correspondence to this author at the Department of Biochemistry and Molecular Biophysics, Box 8231, Washington University School of Medicine, St. Louis, MO 63110.
[§] Department of Pediatrics.
[∥] Department of Biochemistry and Molecular Biophysics.

0006-2960/90/0429-823$02.50/0